International Journal of Automotive Technology, Vol. 5, No. 1, pp. 23–31 (2004)

1229–9138/2004/015–04

EFFECTS OF SKIRT PROFILES ON THE PISTON SECONDARY MOVEMENTS BY THE LUBRICATION BEHAVIORS

S. JANG[1] and J. CHO[2]*

[1]School of Mechanical and Automotive Engineering, Kookmin University, Seoul 136-702, Korea
[2]Graduate School of Atomotive Engineering at Kookmin University, Seoul 136-702, Korea
(*Presently at Korea Institute of Machinery & Materials, KIMM)

(Received 8 September 2003; Revised 24 December 2003)

ABSTRACT–Secondary movements of piston in the bore clearance are closely related to the side impact to the engine block as well as many tribological problems. Some of the major parameters that influence these kinds of movements are piston profile shapes (barrel and flat), piston pin offsets and the magnitudes of bore clearances. In our study, computational investigations are performed about the piston movements in the bore clearance by changing the skirt profiles and piston offsets. In this work, it is found that curved profile and larger offset magnitude to thrust side provide better performance that has low side impact during the engine cycle.

KEY WORDS : Secondary movement of piston, Skirt profile, Piston offset, Side impact, Hydrodynamic lubrication

NOMENCLATURE

a : vertical distance from top of piston skirt to the piston center of mass $[m]$
b : vertical distance from top of piston skirt to the wrist pin $[m]$
c : radial clearance $[m]$
C_g : distance of the piston center of mass from the wrist pin axis $[m]$
C_p : wrist pin offset $[m]$
e_t : eccentricity of piston at the top of skirt $[m]$
e_b : eccentricity of piston at the bottom of skirt $[m]$
F_{hyd} : load capacity of the hydrodynamic fluid film $[N]$
F_G : combustion gas force $[N]$
F_{sx} : lateral inertia force due to piston skirt mass $[N]$
F_{sy} : axial inertia force due to piston skirt mass $[N]$
F_{px} : lateral inertia force due to wrist pin mass $[N]$
F_{py} : axial inertia force due to wrist pin mass $[N]$
F_l : force along the connecting rod $[N]$
F_f : viscous friction force $[N]$
h : oil film thickness $[m]$
I_{pis} : moment of inertia of the piston about its center of mass $[\mathrm{kg}\cdot m^2]$
L : piston skirt length $[m]$
l : connecting rod length $[m]$
M_{hyc} : moment about wrist pin due to the hydrodynamic force $[N\cdot m]$
M_f : moment due to viscous friction force $[N\cdot m]$
M_{IS} : moment due to piston skirt inertia force $[N\cdot m]$
M_{IP} : moment due to wrist pin inertia force $[N\cdot m]$
m_{pis} : piston skirt mass $[kg]$
m_{pin} : wrist pin mass $[kg]$
P_{hyd} : hydrodynamic pressure $[Pa]$
P_G : gas pressure $[Pa]$
R : piston radius $[m]$
r : crank arm length $[m]$
t : time $[s]$
U : piston axial velocity $[m/s]$
X : lateral piston displacement $[m]$
Y : axial piston displacement $[m]$
y : fluid film axial coordinate measured from top of piston skirt $[m]$
α : piston tilt angle $[rad]$
μ : lubricant viscosity $[Pa\cdot s]$
ω : crankshaft rotational speed $[s^{-1}]$
$*$: superscript, dimensionless value

*Corresponding author. e-mail: jangs@kookmin.ac.kr

1. INTRODUCTION

Clearance design is very important to many mechanical elements of moving parts in many aspects. Among the various mechanical components mving with clearance, the performance of piston strongly depends on the skirt profile as well as the magnitude of clearance itself, which in turn decides the endurance life of the piston. In general, tight clearance design makes many tribological

problems with low noise and vibration, while loose clearance design have less friction and wear with larger side impact of piston to cylinder block. Piston movement is under high combustion pressure and sudden change of velocity and its directions. This is the reason that the clearance design of skirt profile greatly influences the tribological problems and side impacts on the cylinder wall (Ohta and Yamamoto, 1987). Therefore, it is necessary to consider both these effects simultaneously for better efficient engine that has low impact vibrations and tribological problems.

In order to investigate the movement of piston in the clearance between piston and cylinder wall, verification of fluid film behaviors due to hydrodynamic lubrication needs to be performed in advance of manufacturing. Many researches have been performed regarding this matter. However, most computations of hydrodynamic lubrication are studied with half Sommerfeld boundary condition (Dursunkaya and Keribar, 1992) that does not consider the real hydrodynamic lubrication condition. In our work, the fluid film pressures are computed with three kinds of piston movements such as sliding, rolling and translation with Reynold's boundary condition (Hamrock, 1995) during an engine cycle. Piston movements are traced in the bore clearance (gap between piston skirt and cylinder wall) by equating the applied forces from combustion pressure and many other inertia forces with fluid film pressure by hydrodynamic lubrication.

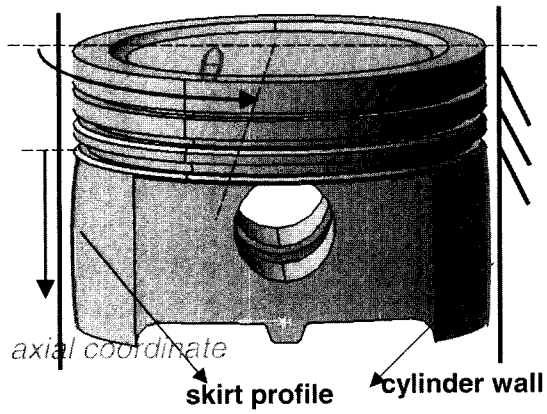

(a) Profile in piston skirt area

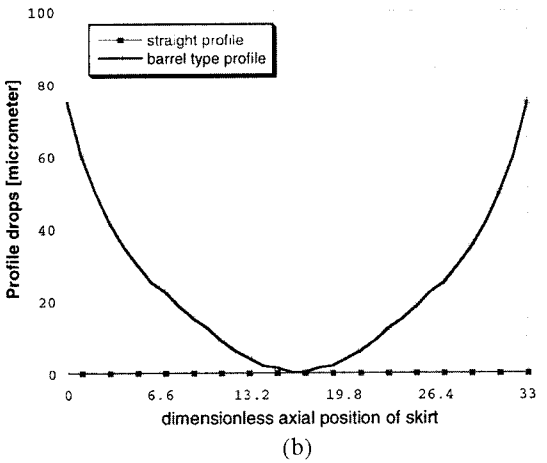

(b)

Figure 1. (b) Comparison of skirt profiles between flat and barrel types of pistons.

2. PISTON SKIRT PROFILE OF FLAT AND BARELL TYPES

Better lubricant film of hydrodynamic lubrication can be made when the sliding direction of moving element is oriented to the narrower space of the gap. Straight profile of piston skirt (flat type) can make lubrication film on the narrower gap side of sliding direction (i.e. thrust side). However, piston have wider gap of sliding direction (i.e. anti-thrust side) on the other side, so the piston can not be supported by the fluid film pressure and sometimes direct impact on the cylinder block occurs with large vibration, so called piston slap. When the skirt profile has curved feature like barrel type, it can be supported by the fluid film pressure on both sides of piston skirts, so that the

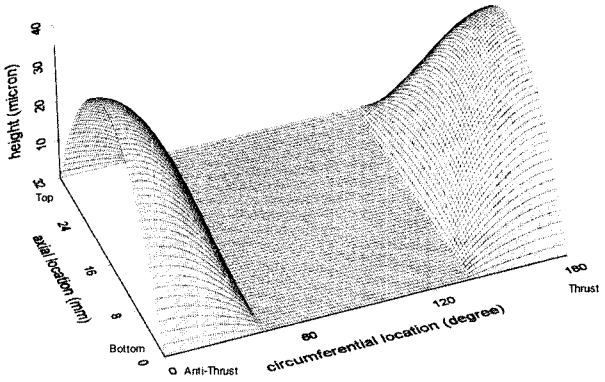

Figure 2. Skirt profiles on thrust and anti-thrust sides of barrel type piston.

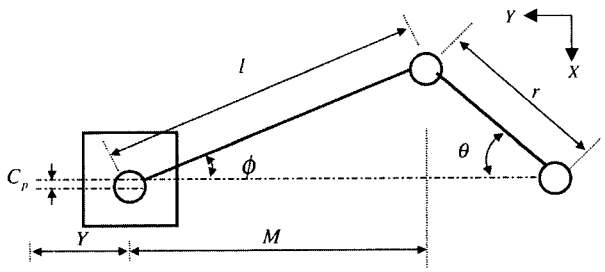

Figure 3. Crank slider mechanism without any clearance movements in the gap between cylinder and piston skirt.

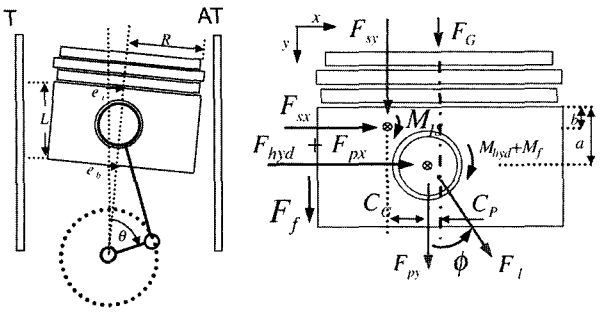

Figure 4. Forces and moments acting on the piston.

direct impact happens less frequently. Figure 1 shows the profile differences between straight and barrel profiles in the area of piston skirt and Figure 2 shows surface shape of barrel type skirt.

3. PISTON SECONDARY MOVEMENTS

Piston system consists of piston, piston pin, connecting rod, crankshaft, etc. Piston slides in the axial direction through cylinder and the displacement of piston (piston primary movement) is expressed in the following form:

$$Y = l(1-\cos\phi) + r(1-\cos\theta) \tag{1}$$

Piston velocity, Equation 2 and acceleration, Equation 3 in the axial direction (y-direction) are obtained by differentiating the above Equation (1).

$$U = \frac{(r\sin\theta + C_p)(r\omega\cos\theta)}{M} + r\omega\sin\theta \tag{2}$$

$$\ddot{Y} = \frac{(r\cos\theta\omega)^2}{M} - \frac{(r\sin\theta + C_P)(r\sin\theta\omega^2)}{M} + \frac{(r\sin\theta + C_P)^2(r\cos\theta\omega)^2}{M^3} + r\cos\theta\omega^2 \tag{3}$$

However, piston translates and rotates in the lateral direction, which is called as secondary movement of piston, and if the clearance is large, the piston moves laterally with low friction but gives high impact on the cylinder wall. On the other hand, if the clearance is small, it gives low impact but produces high frictional power loss and many tribological problems. In order to precisely verify these effects, it is necessary to find out the forces acting on the piston components, such as piston skirt, piston pin, connecting rod, etc. Figure 4 shows the forces on the piston components under the operating condition.

The forces in the x and y directions are shown in Equations (4) and (5) and moment equation piston rotating around piston pin is shown in Equation (6).

$$\sum F_y = F_G + F_f + F_{py} + F_{sy} + F_l\cos\phi = 0 \tag{4}$$

$$\sum F_x = F_{hyd} + F_{px} + F_{sx} - F_l\sin\phi = 0 \tag{5}$$

$$\sum M_{pin} = M_{hyd} + M_f + M_{IS} + F_{sx}(a-b) - F_{sy}C_g + F_GC_p = 0 \tag{6}$$

With Equations (4) and (5), new force equilibrium, Equation (7) is obtained by deleting the force component along the connecting rod, F_l.

$$-F_{px} - F_{sx} = F_{hyd} + F_f\tan\phi + F_{Wall} \tag{7}$$

Lateral Force F_{wall} is defined according to the angle of con-rod rotation ϕ as in Equation (8).

$$F_{Wall} = (F_G + F_{py} + F_{sy})\tan\phi \tag{8}$$

Similarly, the moment Equation (6) is rearranged as in Equation (9).

$$-M_{IS} - F_{sx}(a-b) = M_{hyd} + M_f + M_{Wall} \tag{9}$$

and the magnitude of moment due to lateral force, M_{wall} is defined as Equation (10).

$$M_{Wall} = F_GC_p - F_{sy}C_g \tag{10}$$

The axial forces by the piston and piston pin movements are expressed by the following Equation (11) and (12).

$$F_{sy} = -m_{pis}\ddot{Y} \tag{11}$$

$$F_{py} = -m_{pin}\ddot{Y} \tag{12}$$

The translational accelerations, top and bottom sides of piston about the piston pin is obtained by geometrical relationship shown in Figure 5 by the following Equations (13) and (14).

$$\frac{\ddot{e}_t - \ddot{e}_b}{L} = \frac{\ddot{e}_t - \ddot{e}_p}{a} \tag{13}$$

$$\ddot{e}_p = \ddot{e}_t + \frac{a}{L}(\ddot{e}_b - \ddot{e}_t) \tag{14}$$

The acceleration of piston skirt mass center, Equation (15) is obtained in the same way as above:

$$\ddot{e}_c = \ddot{e}_t + \frac{b}{L}(\ddot{e}_b - \ddot{e}_t) \tag{15}$$

The inertia forces in the x direction by the translational and rotational movements of piston are expressed by the following forms:

$$F_{sx} = -m_{pis}\left(\ddot{e}_t - \frac{a}{L}(\ddot{e}_b - \ddot{e}_t)\right) \tag{16}$$

$$F_{px} = -m_{pis}\left(\ddot{e}_t - \frac{b}{L}(\ddot{e}_b - \ddot{e}_t)\right) \tag{17}$$

$$M_{IS} = \frac{I_{pis}(\ddot{e}_t - \ddot{e}_b)}{L} \tag{18}$$

In order to find out the motions of piston in the bore clearance, system equation from the above Equations (4)–(18) can be expressed as in Equation (19).

$$\begin{bmatrix} m_{pis}\left(1-\frac{b}{L}\right)+m_{pin}\left(1-\frac{a}{L}\right) & m_{pis}\frac{b}{L}+m_{pin}\frac{a}{L} \\ \frac{I_{pis}}{L}+m_{pis}(a-b)\left(1-\frac{a}{L}\right) & -\frac{I_{pis}}{L}+m_{pis}(a-b)\frac{b}{L} \end{bmatrix} \begin{bmatrix} \ddot{e}_t \\ \ddot{e}_b \end{bmatrix} = \begin{bmatrix} F_{hyd}+F_f\tan\phi+F_{Wall} \\ M_{hyd}+M_j+M_{Wall} \end{bmatrix} \tag{19}$$

4. HYDRODYNAMIC LUBRICATION IN THE BORE CLEARANCE

The force equilibrium between side force by piston inertia and fluid film pressure due to hydrodynamic lubrication is computed at each time step (total 720 steps) during one engine cycle by tracing the upper and lower positions of piston as it is done by Dursunkaya (1992). The forces on the piston come from combustion pressure, acceleration of piston components and fluid film pressures (Equation 20), by three kinds of movements such as translation, sliding and rotation. Many other researches have performed the computation of hydrodynamic lubrication pressure with half Sommerfeld boundary condition for three kinds of movements which have many computational simplifications. In our study, we impose Reynolds boundary condition for the computation of fluid film pressure, which meets more physical conditions of piston movements as it is shown in Figure 6. In the region of cavitation, none of the movements can make hydrodynamic lubrication pressures.

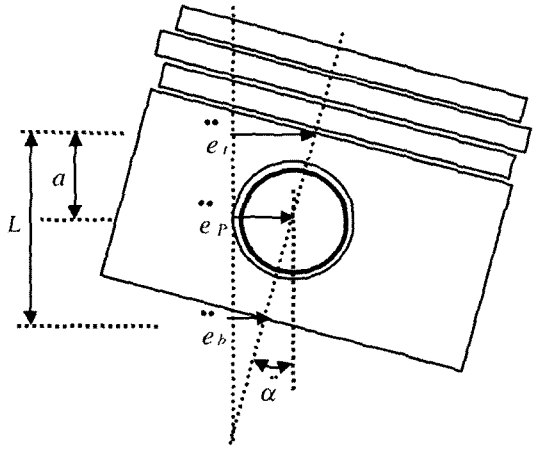

Figure 5. Lateral accelerations of top, bottom and piston pin positions.

$$\frac{\partial}{\partial y^*}\left(h^{*3}\frac{\partial p^*}{\partial y^*}\right)+\frac{\partial}{\partial\theta}\left(h^{*3}\frac{\partial p^*}{\partial\theta}\right) = -U^*\left(\frac{(\varepsilon_b-\varepsilon_t)\cos\theta}{L^*}+\frac{\partial f(y^*,\theta)}{\partial y^*}\right) +\beta\left(\dot{\varepsilon}_t\cos\theta+(\dot{\varepsilon}_b-\dot{\varepsilon}_t)\frac{y^*}{L^*}\cos\theta\right) \tag{20}$$

where, the dimensionless form of film thickness is expressed by the following Equation (21):

$$h^* = 1+\varepsilon_t\cos\theta+\frac{y^*(\varepsilon_b-\varepsilon_t)\cos\theta}{L^*}+f(y^*,\theta) \tag{21}$$

Total pressure p^* is obtained by the summation of three kinds of movements as Equation (22) according to linear characteristics of partial differential equation solution.

$$p^* = -U^*p_1^*+\dot{\varepsilon}_tp_2^*+(\dot{\varepsilon}_b-\dot{\varepsilon}_t)p_3^* \tag{22}$$

for the pressure of p_1^* piston sliding:

$$\frac{\partial}{\partial y^*}\left(h^{*3}\frac{\partial p^*}{\partial y^*}\right)+\frac{\partial}{\partial\theta}\left(h^{*3}\frac{\partial p^*}{\partial\theta}\right) = \left(\frac{(\varepsilon_b-\varepsilon_t)\cos\theta}{L^*}+\frac{\partial f(y^*,\theta)}{\partial y^*}\right) \tag{23}$$

for the pressure p_2^* of translation:

$$\frac{\partial}{\partial y^*}\left(h^{*3}\frac{\partial p^*}{\partial y^*}\right)+\frac{\partial}{\partial\theta}\left(h^{*3}\frac{\partial p^*}{\partial\theta}\right) = \beta\cos\theta \tag{24}$$

for the pressure p_3^* of rotation:

$$\frac{\partial}{\partial y^*}\left(h^{*3}\frac{\partial p^*}{\partial y^*}\right)+\frac{\partial}{\partial\theta}\left(h^{*3}\frac{\partial p^*}{\partial\theta}\right) = \frac{y^*}{L^*}\beta\cos\theta \tag{25}$$

The pressure components such as p_1^*, p_2^*, p_3^* and total pressure p_T^* are computed by applying Reynolds boundary condition, which has not been considered in many previous studies using half sommerfeld condition. (Dursunkaya and Keribar, 1992) That is, if hydrodynamic lubricant (total pressure) p_T^* does not exist on the skirt surface in some area region, then any pressure component, p_1^*, p_2^* and p_3^* is not computed. All the simulations in our study are based on this assumption, which predicts more realistic results.

The force and moment by the piston on the cylinder wall due to the hydrodynamic lubrication pressure is obtained after integrating the pressure over the contact area as shown in Equations (26) and (27).

$$F_{hyd}^* = 2\int_0^{L^*}\int_0^{\pi}p^*\cos\theta\,d\theta\,dy \tag{26}$$

$$M_{hyd}^* = 2\int_0^{L^*}\int_0^{\pi}p^*(a^*-y^*)\cos\theta\,d\theta\,dy \tag{27}$$

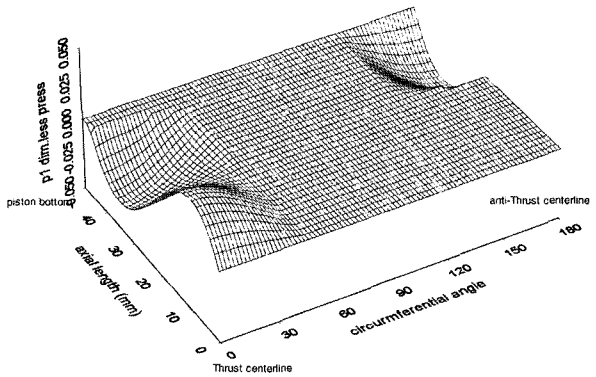

(a) Pressure distribution for p_1 component between the centerlines of thrust and anti-thrust sides by Reynold's boundary condition

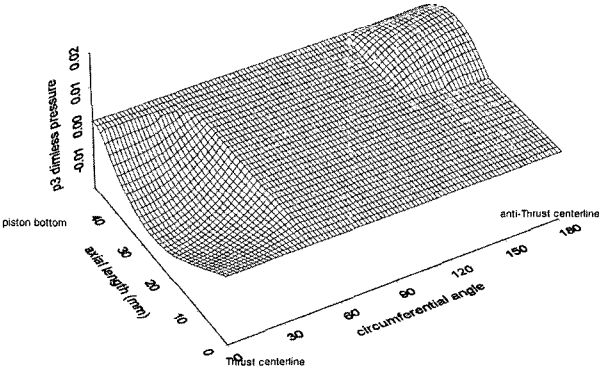

(c) Pressure distribution for p_3 component between the centerlines of thrust and anti-thrust sides by Reynold's boundary condition

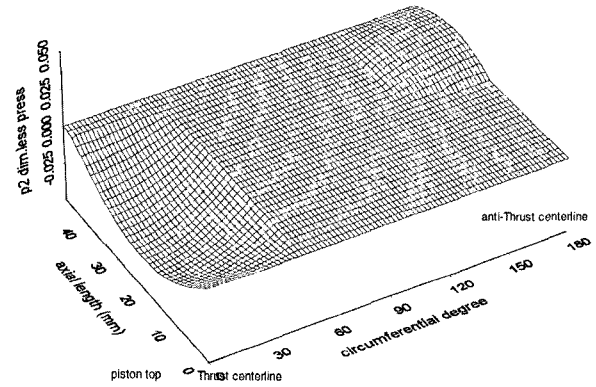

(b) Pressure distribution for p_2 component between the centerlines of thrust and anti-thrust sides by Reynold's boundary condition

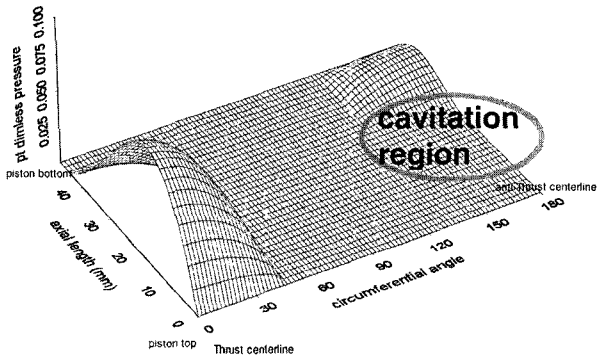

(d) Pressure distribution for total pressure p_T between the centerlines of thrust and anti-thrust sides by Reynold's boundary condition

Figure 6. Pressure shapes of each component and total pressure using Reynolds boundary condition for barrel type piston at crank angle 160°, engine speed 4000 *rpm*, $\varepsilon_t = -0.46445$, $\varepsilon_b = 0.87957$, $d\varepsilon_t/dt^* = 0.02121$ and $d\varepsilon_b/dt^* = 0.001048$ ($t^* = \omega t$).

The hydrodynamic pressure is decomposed into three components as in Equations (28) and (29). Therefore, force and moment by hydrodynamic lubrication are expressed by the following Equations with applying cavitation boundary condition.

$$F^*_{hyd} = -U^* F^*_1 + \dot{\varepsilon}_t F^*_2 + (\dot{\varepsilon}_b - \dot{\varepsilon}_t) F^*_3 \tag{28}$$

$$M^*_{hyd} = -U^* M^*_1 + \dot{\varepsilon}_t M^*_2 + (\dot{\varepsilon}_b - \dot{\varepsilon}_t) M^*_3 \tag{29}$$

The corresponding friction force and moment by viscous resistance of fluid film in the bore clearance are computed by the following Equations (30) and (31).

$$F^*_f = 2\iint\left(3h^* \frac{\partial p^*}{\partial y^*} + \frac{U^*}{h^*}\right) d\theta dy^* \tag{30}$$

$$M^*_f = -2\iint\left(3h^* \frac{\partial p^*}{\partial y^*} + \frac{U^*}{h^*}\right) \cos\phi \, d\theta dy^* \tag{31}$$

The top and bottom side accelerations of piston ($\ddot{e}_t$, $\ddot{e}_b$) are computed by finite difference method for time step using the values of (e_t, e_b) and the Equation (19) is simplified by the following form.

$$\begin{bmatrix} F_{hyd}(\dot{e}_t, \dot{e}_b, e_t, e_b) \\ M_{hyd}(\dot{e}_t, \dot{e}_b, e_t, e_b) \end{bmatrix} - \begin{bmatrix} F_{SUM} \\ M_{SUM} \end{bmatrix} = \begin{bmatrix} 0 \\ 0 \end{bmatrix} \tag{32}$$

where, F_{SUM}, M_{SUM} are the summation of inertia and external forces and moments by the piston. The Jacobian matrix Equation (32) is expressed by the following Equation (33) in order to get the next time step values of $\dot{\varepsilon}_t$ and $\dot{\varepsilon}_b$.

$$\begin{bmatrix} \dot{e}_t \\ \dot{e}_b \end{bmatrix}^{(i+1)} = \begin{bmatrix} \dot{e}_t \\ \dot{e}_b \end{bmatrix}^{(i)} - \begin{bmatrix} \dfrac{\partial F_{hyd}}{\partial \dot{e}_t} & \dfrac{\partial F_{hyd}}{\partial \dot{e}_b} \\ \dfrac{\partial M_{hyd}}{\partial \dot{e}_t} & \dfrac{\partial M_{hyd}}{\partial \dot{e}_b} \end{bmatrix} \begin{bmatrix} F^{(i)}_{hyd} - F_{SUM} \\ M^{(i)}_{hyd} - M_{SUM} \end{bmatrix} \tag{33}$$

The values of $\dot{e}_t$, $\dot{e}_b$ are computed by Newton-Raphson method and once these values are determined, the next step for e_t, e_b is computed by the following procedure.

$$e_t(t+\Delta t) = e_t(t) + \Delta t\dot{e}_t$$
$$e_b(t+\Delta t) = e_b(t) + \Delta t\dot{e}_b \quad (34)$$

5. RESULTS

Regarding the effects of bore clearance size on the piston movements, it is found that large bore clearance can cause more side impact to the cylinder wall as it is shown in Figure 7, even if hydrodynamic pressure between skirt and cylinder wall exists on any spatial gap features. The upper and lower locations of piston agitate in wider range for the piston profile of c=60 μm clearance than for the piston of c=20 μm clearance.

The piston movements are more aligned with the piston large offset (0.6 mm) magnitude than with small

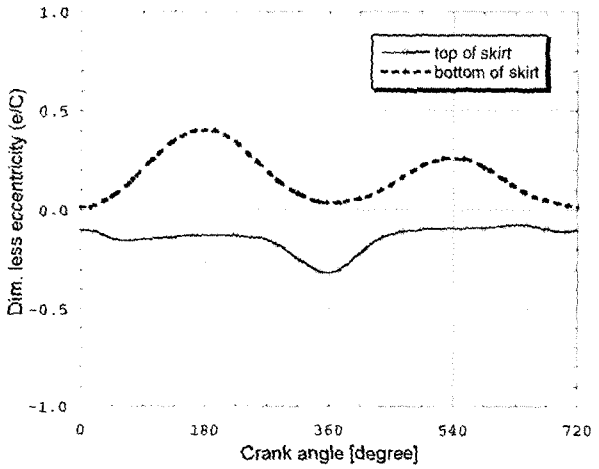

(a) Bore clearance c=20μm

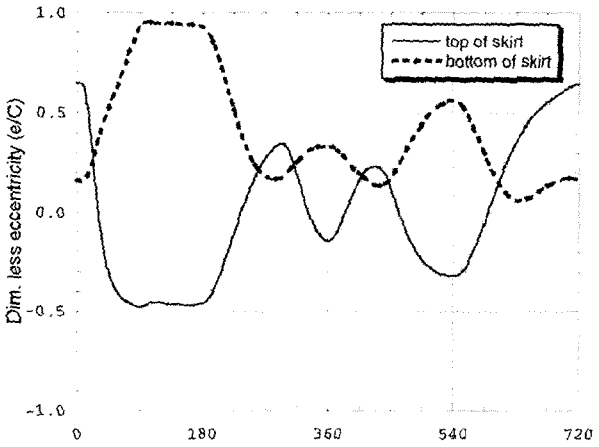

(b) Bore clearance c=60μm

Figure 7. Piston movements according to the clearance sizes at 0.2 mm offset and 4000 rpm in flat type skirt.

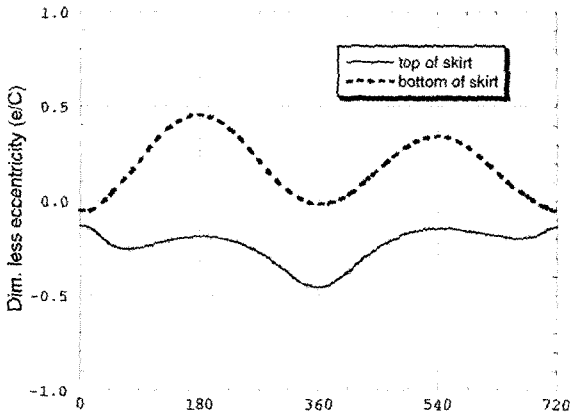

(a) c=20μm, offset=0.2mm, flat type

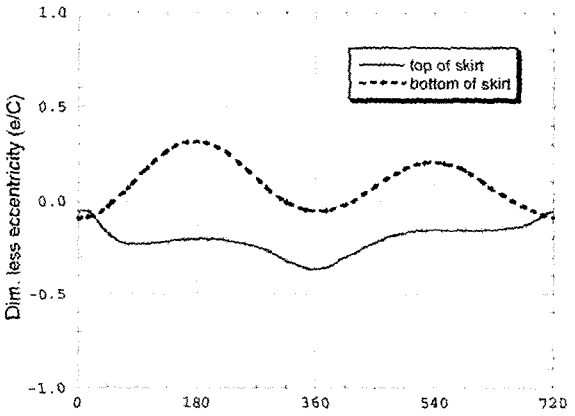

(b) c=20μm, offset=0.4mm, flat type

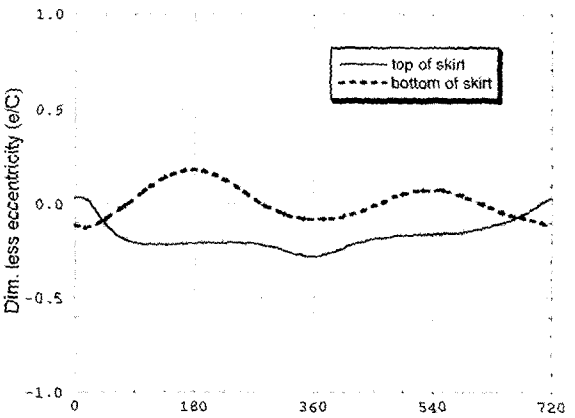

(c) c=20 μm, offset=0.6mm, flat type

Figure 8. Piston movements of flat type piston for different offset sizes at 2000 rpm.

offset piston (0.2 mm) for flat type piston as shown in Figure 8(a), (b) and (c).

In order to find out the skirt profile effects, the piston of barrel type has more rotating motions (Figure 9(b)), especially at the location of bottom dead center (crank angle 360°) than the piston of flat type profile (Figure 9(a)). This means that the piston of barrel type skirt has less impact than the piston of flat type skirt, because it has rolling motion rather than direct impact when the piston changes its sliding directions.

Comparing the patterns of piston path line in the bore clearance between flat and barrel types, flat type piston has more simultaneous translational motions in top and bottom sides (Figure 10) than barrel type piston. In case of barrel type piston, the motion has more rotational movements (Figure 11) as explained previously. These kinds of motions by flat type skirt mean that piston has more possibilities of direct impacts to the cylinder side. All of the simulations performed in our study shows that these kinds of movements are general patterns. These results prove that barrel type piston has better vibrational performance due to hydrodynamic lubrication effects supporting both sides (thrust and anti-thrust sides).

Over all the period of one cycle, the rotational movements of piston around piston pin has wider rotating

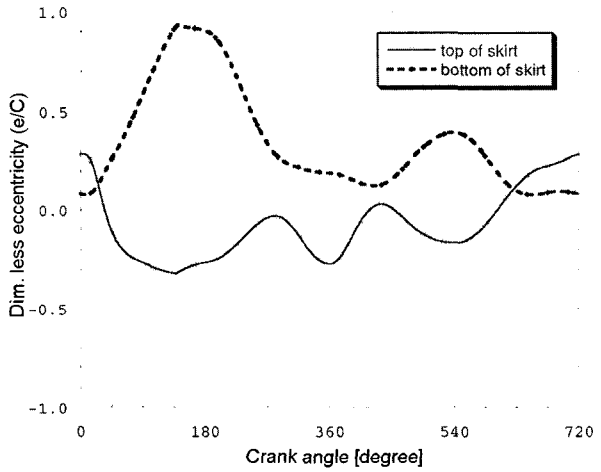

(a) Flat skirt type and bore clearance c=40μm.

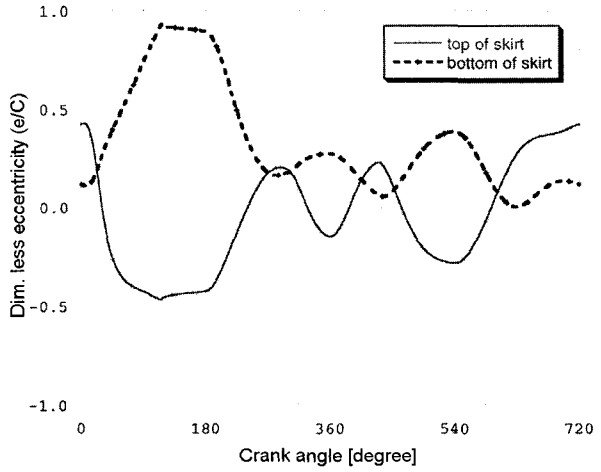

(b) Barrel skirt type and bore clearance c=40μm

Figure 9. Piston movements according to skirt profiles at 0.2 mm offset and 4000 rpm.

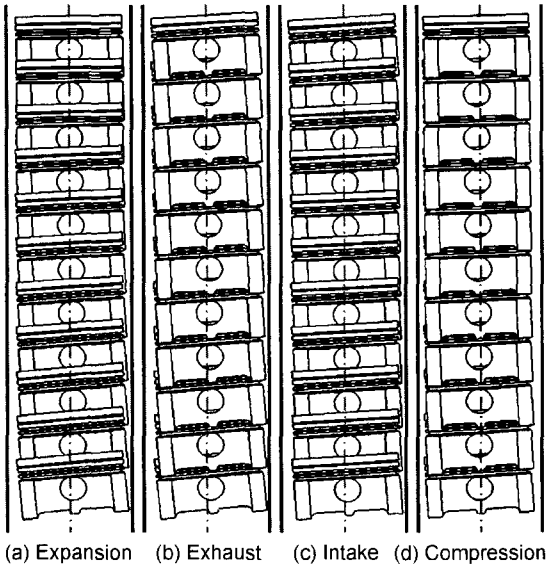

Figure 10. Piston pathline of flat profile piston in the clearance during one according to piston pin offset of 0.2 mm at 4000 rpm and c=20 μm.

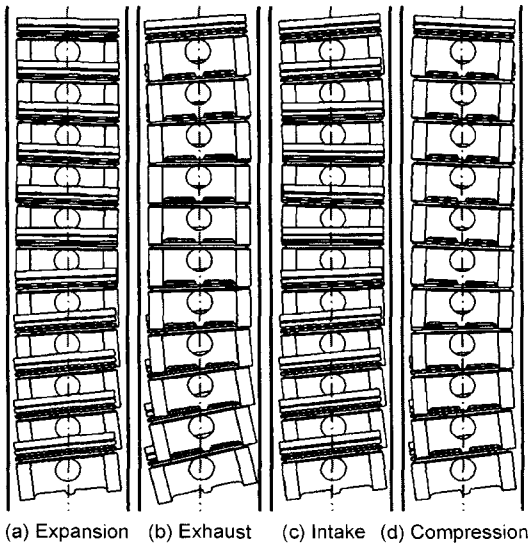

Figure 11. Piston pathline of barrel profile piston in the clearance during one cycle according to piston pin offset of 0.2 mm at 4000 rpm and c=40 μm.

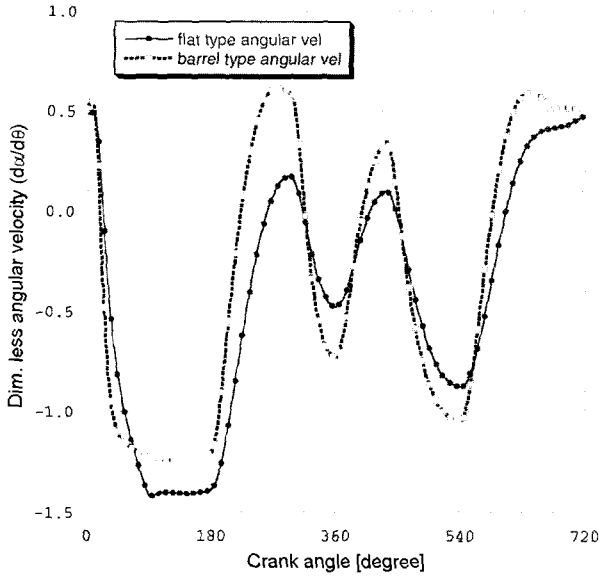

Figure 12. Rotational angle around piston pin for flat and barrel type pistons with c=60 μm, 0.2 mm offset, 4000 rpm.

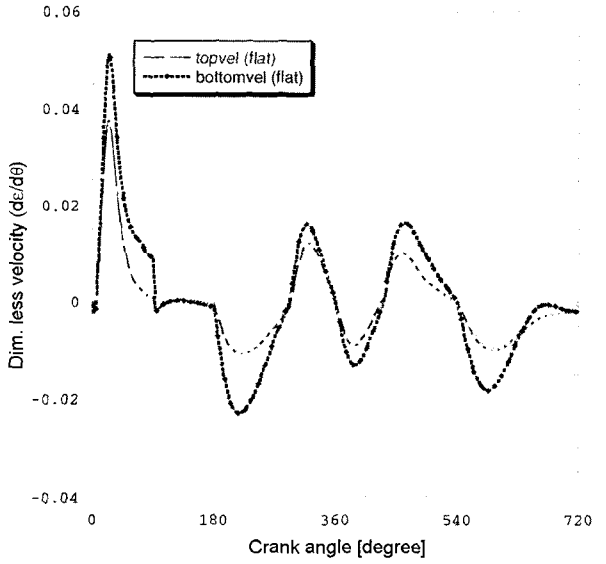

Figure 13. Translational velocity of top and bottom sides for flat profile piston with c=60 μm, 0.2 mm offset, 4000 rpm.

angle range in barrel type than in flat type (Figure 12). As it was previously explained, barrel type piston has rolling movement as the piston approaches the cylinder wall. Translational velocity is another factor to find out the characteristics of piston movements. More investigation of piston movements in the clearance will exactly verify the characteristics of piston movements. During the expansion stroke, the velocities of top and bottom sides

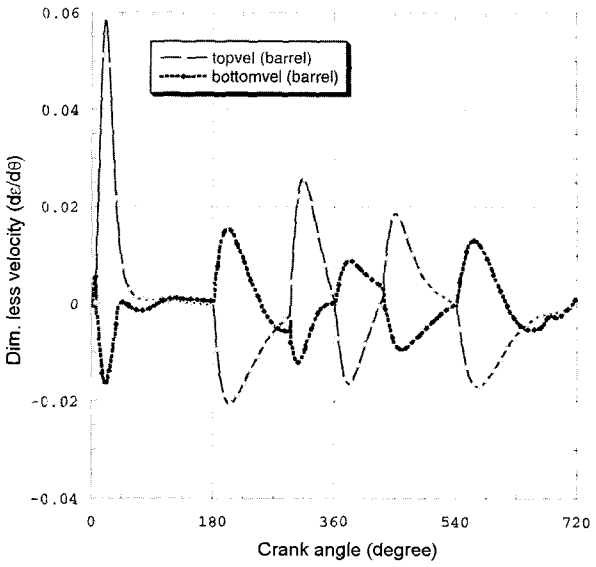

Figure 14. Translational velocity of top and bottom sides for barrel profile piston with c=60 μm, 0.2 mm offset, 4000 rpm.

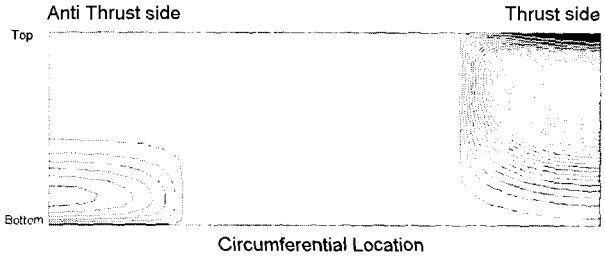

Figure 15. Pressure distribution at 30° crank angle (Flat Skirt, Max Pressure 50.05 bar).

in flat type have almost the same magnitude as each other, which means piston gives impact on the cylinder wall (Figure 13). The translational velocity directions are unique with barrel type piston, because the directions of top and bottom sides are opposite to each other during expansion stroke (crank angle 0°–180°, Figure 14), where it has the most severe period for vibrational and

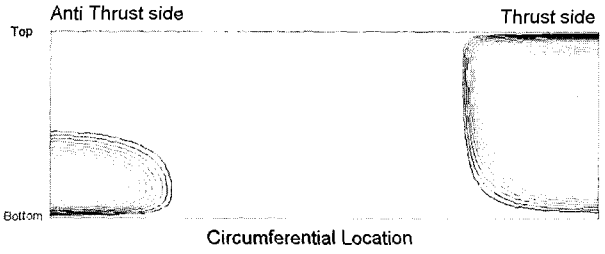

Figure 16. Pressure distribution at 30° crank angle (Barrel Skirt, Max Pressure 55.09 bar).

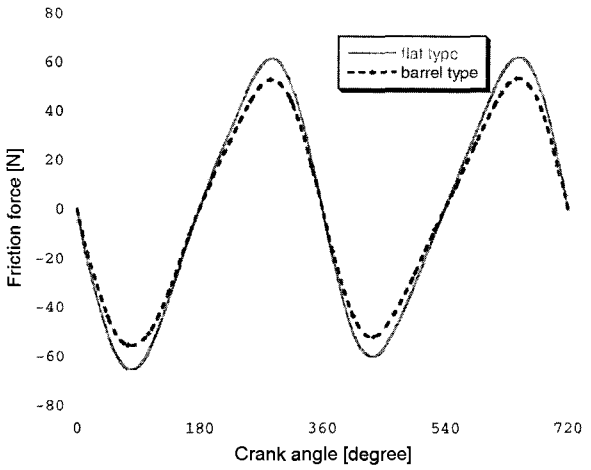

Figure 17. Friction forces on the piston skirt by changing skirt profiles.

tribological behaviors.

As far as the viscous friction is concerned without asperity contacts in the numerical modeling, the pressure distributions over the skirt area for flat type piston has lower values than that for barrel type piston (Figures 15 and 16). This means that flat type piston has higher film thickness than barrel type piston for the same applied load. Therefore, the viscous friction in case of flat type has higher value that in case of barrel type as shown in Figure 17.

6. CONCLUSION

Computational study of piston movement in the bore clearance has been performed in order to verify the skirt profile effects. Based on the assumption of hydrodynamic lubrication theory, hydrodynamic lubrication pressure shapes over the skirt area are computed and compared among the results. According to the analysis of velocities of piston top and bottom sides, it is found that barrel type of skirt profile has better performance of clearance movements than flat type.

ACKNOWLEDGEMENT–This work was supported by 2003 Kookmin University Research Fund.

REFERENCES

Dursunkaya, Z. and Keribar, R. (1992). A comprehensive model of piston skirt lubrication. *SAE Paper No.* 920483.

Dursunkaya, Z. and Keribar, R. (1992). Simulation of secondary dynamics of articulated and conventional piston assemblies. *SAE Paper No.* 920484.

Hamrock B. J. (1995). *Fundamentals of Fluid Film Lubrication*. McGraw-Hill. New York.

Ohta, K. and Yamamoto, K. (1987). Piston slap induced noise and vibration of internal combustion engines. *SAE Paper No.* 8709907.